EasyChair Preprint

№ 8791

A Frequency Adaptive Multi-Rate Repetitive Control for Single-Phase Grid-Connected Inverter

Kaiyue Liu, Qiangsong Zhao, Gong Zhang and Bin Wang

September 5, 2022

A Frequency Adaptive Multi-rate Repetitive Control for Single-phase Grid-connected Inverter

1st Kaiyue Liu
School of Electronic and Information, Zhongyuan University of Technology
Zhengzhou, China
lumina2021@163.com

2nd Qiangsong Zhao
School of Electronic and Information, Zhongyuan University of Technology
Zhengzhou, China
zhaoqiangsong@126.com

3rd Gong Zhang
School of Electronic and Information, Zhongyuan University of Technology
Zhengzhou, China
zhgong068@126.com

4th Bin Wang
School of Electronic and Information, Zhongyuan University of Technology
Zhengzhou, China
wangbin251x@163.com

***Abstract*—In order to improve the harmonic suppression capability of the traditional repetitive control (CRC) when the grid frequency fluctuates and reduce the computational burden of the digital system, a frequency adaptive multi-rate repetitive control (FAMRC) scheme is proposed in this paper. FAMRC is composed of a multi-rate repetitive control (MRC) with low sampling rate and a Farrow structure fractional delay (FD) filter based on Taylor series expansion. After the stability analysis and parameter design of the system, FAMRC can achieve lower tracking error and faster convergence speed, accurately approximate the FD generated when the fundamental frequency of the power grid fluctuates, and achieve good frequency adaptation. Simulations verify the effectiveness of the proposed strategy.**

Keywords—repetitive control; multi-rate; fractional delay; frequency adaptation

I. INTRODUCTION

Distributed generation (DG) is a kind of clean energy with strong adaptability to the environment. However, many non-linear power electronic switching devices are used in distributed generation, which will inject a large amount of harmonic current into the grid system and reduce the power quality[1]. Grid-connected inverter is the interface unit of distributed generation system to transmit power to the grid. In order to reduce the harmonic content of the grid current of the inverter, L-type filter and LCL-type filter are usually used to suppress the high frequency harmonic at the switching frequency of the grid current. Under the same harmonic suppression requirements, LCL filter is widely used because of its smaller actual volume and lower cost, which can better suppress grid current harmonics[2],[3].

For the suppression of low-frequency harmonics in grid current, many control methods have been proposed. Among them, repetitive control (RC)[4] is widely used because it can realize the static error-free tracking and disturbance rejection of fundamental and harmonics of sinusoidal signals. However, when the traditional repetitive control (CRC) is implemented in digital, the sampling rate of the repetitive controller and the switching frequency of the inverter power device are often 10kHz or even higher, which makes the memory consumption of the controller too large and the calculation burden too heavy. For this reason, multiple rate repetitive control (MRC)[5],[6] has been proposed, in which the repetitive controller is set in a low sampling frequency environment, and the feedback part of the grid-connected current still adopts high sampling rate. Compared with CRC, the memory consumption and calculation times of MRC controller in each sampling period are greatly reduced[7]. Previous work has shown that MRC can maintain the same convergence rate and total harmonic distortion (THD) as CRC, and CRC is a special case when MRC sampling factor $m = 1$.

In the distributed generation system, the grid frequency tends to fluctuate, and the resonant frequency of RC will deviate from the actual grid frequency, resulting in a significant decrease in the compensation ability of the system[8],[9]. When the delay beat number N (the ratio of sampling frequency to fundamental frequency) is a fraction, it cannot be realized in the digital system. If N is rounded to the nearest integer, the gain of repetitive control will be reduced and the harmonic suppression ability of the system will be decline. In this case, reference [10] proposed a high-order repetitive control (HORC), which can improve the robustness of the system in the case of small frequency changes. Reference [11] guarantees that N is an integer by changing the sampling frequency, but the constant change of sampling frequency will make the controller design complex. In [12], FD was approximated by FIR filter based on Lagrange interpolation to obtain any numerical delay N, which improved the adaptive ability of repetitive control.

However, the FIR filter based on Lagrange interpolation needs to recalculate the coefficients of $M + 1$(M is the order of FIR filter) sub-filters when updating the coefficients, which increases the computational burden[13]. Therefore, in this paper, a frequency adaptive multi-rate repetitive control (FAMRC) consisting of a Farrow structure FD filter based on Taylor series expansion, is proposed. Each subfilter of the Farrow structure FD filter is designed offline in advance. For the new FD, only the fractional N decimal value is adjusted, which greatly reduces the computational burden of the controller.

This work was supported in part by the National Natural Science Foundation of China under Grant 61973157.

II. LCL-TYPE SINGLE-PHASE GRID-CONNECTED INVERTER MODEL

The model of LCL-type single-phase grid-connected inverter is shown in Fig.1. E_d is dc bus voltage, u_{inv} is inverter output voltage. v_g is the grid voltage, i_g is the grid current, and i_{ref} is the reference current. L_1 and L_2 are filter inductance, R_1 and R_2 are equivalent series resistance. C is the filter capacitor and R is the series resistance of the capacitor to suppress the resonance peak generated by LCL filter.

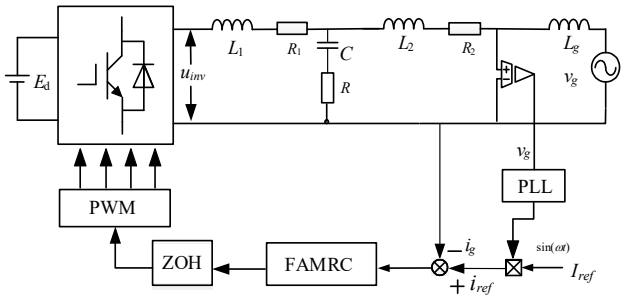

Fig. 1. LCL-type single-phase grid-connected inverter model

Ignoring the equivalent resistance of the inductors, the transfer function from the input voltage u_{inv} to the grid current i_g is

$$P(s)=\frac{CRs+1}{CL_1L_2s^3+C(L_1+L_2)Rs^2+(L_1+L_2)s} \tag{1}$$

Table I shows the parameters of LCL-type single-phase grid-connected inverter. With parameters, (1) can be obtained by discretization

$$P(z)=\frac{0.006135z^2+0.004307z-0.002401}{z^3-2.005z^2+1.493z-0.4879} \tag{2}$$

TABLE I. PARAMETERS OF THE LCL-TYPE SINGLE-PHASE GRID-CONNECTED INVERTER

Parameters	value
dc bus voltage E_d/V	380
fundamental frequency f_0/Hz	50
switching frequency f_{sw}/kHz	10
sampling frequency f_s/kHz	10
inductance on inverter side L_1/mH	3.8
L_1 equivalent resistance R_1/Ω	0.48
network side inductance L_2/mH	2.2
L_2 equivalent resistance R_2/Ω	0.32
filter capacitor C/μF	10
Passive damping resistor R/ kHz	10

III. FREQUENCY ADAPTIVE MULTI-RATE REPETITIVE CONTROL

A. MRC

Fig. 2 shows the block diagram of a conventional plug-in MRC system. In the figure, the sampling period of the grid current feedback system is T_s, $E(z)$ is the error between the reference signal $i_{ref}(z)$ and the grid current $i_g(z)$. In order to prevent the distortion of $E(z)$ signal outside the Nyquist frequency when entering the repetitive controller with low sampling rate, the anti-spectral aliasing filter $F_1(z)$ is often used to intercept the signal in the $|\omega| > \pi / T_m$ part, and the signal $E(z_m)$ is obtained by down-sampling as the input of RC. The output $U_r(z_m)$ of RC is up-sampled by zero-order holder (ZOH) to obtain $U_r(z)$, and then an anti-imaging filter $F_2(z)$ with cutoff frequency less than π / T_m is connected to prevent distortion. $G_{pi}(z)$ is a proportional integral controller for stabilizing the closed-loop control system. $P(z)$ is the equivalent controlled object of LCL system, and $u_g(z)$ is the disturbance source.

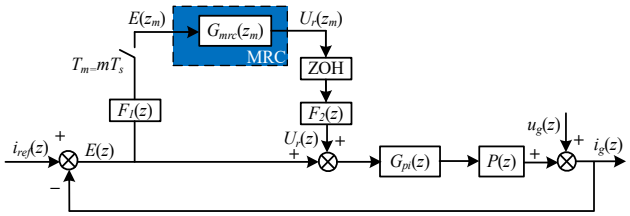

Fig. 2. Plug-in MRC system

The sampling period of RC is T_m, which is m times of T_s, and m is the sampling factor. The relationship between the two sampling rates is

$$T_m = mT_s\,;\, z=e^{sT_s}\,;\, z_m=e^{sT_m}=z^m \tag{3}$$

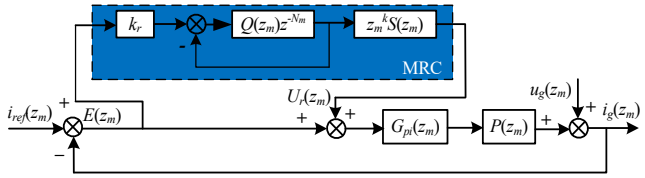

Fig. 3. Equivalent single-rate control system

In order to simplify the analysis, the multi-rate system is transformed into an equivalent single-rate system with low sampling rate, and the structure is shown in Fig.3. $G_{pi}(z_m)$ and $P(z_m)$ are the equivalent transfer functions of PI controller and controlled object at low rates, respectively; k_r is the internal mode gain; $Q(z_m)$ is used to improve the robustness of RC; $N_m = T_g / T_m$, T_g is the fundamental frequency period of reference signal and disturbance signal. $S(z_m)$ is a low-pass filter used to accelerate the high-frequency amplitude attenuation of the controlled object; z_m^k is the phase-lead compensation, which is used to compensate the phase lag of the control system. The influence of $F_1(z)$, downsampling link, zero order holder and $F_2(z)$ on the system can also be compensated by the z_m^k.

The transfer function of MRC is

$$G_{mrc}=k_r\frac{z_m^{-N_m}Q(z_m)}{1-z_m^{-N_m}Q(z_m)}S(z_m)z_m^k \tag{4}$$

B. Farrow structure FD Filter design based on Taylor series

When the grid frequency fluctuates and m takes different values, N_m may be a fraction, which can be divided into integer part D and fractional part d, $z_m^{-N_m}=z_m^{-D}z_m^{-d}$. FD transfer function z_m^{-d} can be expanded to a polynomial about d by Taylor series[14].

$$a_n(d) = z_m^{-\mathrm{d}} = e^{-j\omega md} = \sum_{k=0}^{M} \frac{(-j\omega m)^k}{k!}(d)^k \tag{5}$$

Where, $0 \leqslant d < 1$.

FD filter can be expressed as

$$G_d(z_m) = \sum_{n=0}^{S} a_n(d) z_m^{-n} \tag{6}$$

Where S is the order of the FD filter and $a_n(d)$ is the polynomial of d.

Substitute (5) into (6), Farrow [15] FD filter $G_d(z^m)$ can be obtained

$$G_d(z_{\mathrm{m}}) = \sum_{k=0}^{M}\sum_{n=0}^{S} a_{nk} z_m^{-n} d^k = \sum_{k=0}^{M} L_k(z_m) d^k \tag{7}$$

$L_k(z^m)(k = 0, 1, \ldots, M)$ is the k subfilter in $G_d(z_m)$.

Usually choose $S = M$, subfilter calculation formula based on Lagrange interpolation method is as follows[16],[17]:

$$U = \begin{bmatrix} 0^0 & 0^1 & 0^2 & \cdots & 0^S \\ 1^0 & 1^1 & 1^2 & \cdots & 1^S \\ 2^0 & 2^1 & 2^2 & \cdots & 2^S \\ \vdots & \vdots & \vdots & \vdots & \vdots \\ M^0 & M^1 & M^2 & \cdots & M^S \end{bmatrix} \tag{8}$$

$$z_{sub} = \begin{bmatrix} 1 & z_m^{-1} & z_m^{-2} & \cdots & z_m^{-M} \end{bmatrix}^T \tag{9}$$

$$f_{sub} = U^{-1} z_{sub} = \begin{bmatrix} L_0(z_m) & L_1(z_m) & L_2(z_m) & \cdots & L_M(z_m) \end{bmatrix}^T \tag{10}$$

In the formula, f_{sub} is a subfilter matrix, z_{sub} is a delay operator matrix, U is a Vandermon matrix. For different fractional delay z^{-d}, the amplitude response of the first and second order FD filters based on Lagrange interpolation method is shown in Fig. 4. It can be seen that when the sampling frequency is 10kHz (that is, the Nyquist frequency is 5kHz), the bandwidth of the first-order FD filter is 50% (2500/5000) of the Nyquist frequency, and the bandwidth of the second-order FD filter is 63.5% (3175/5000) of the Nyquist frequency. It shows that the FD filter based on the Taylor series expansion Farrow structure can effectively approximate the fractional delay z^{-d}. Generally, the first-order FD is sufficient to provide sufficient bandwidth to compensate harmonic distortion, but higher-order FD can further reduce the error. In this paper, the order $M = 2$.

Thus, the transfer function of FAMRC consisting of the Farrow structured FD filter based on the Taylor series is

$$G_{famrc} = k_r \frac{z_m^{-D} G_d(z_m) Q(z_m)}{1 - z_m^{-D} G_d(z_m) Q(z_m)} S(z_m) z_m^k \tag{11}$$

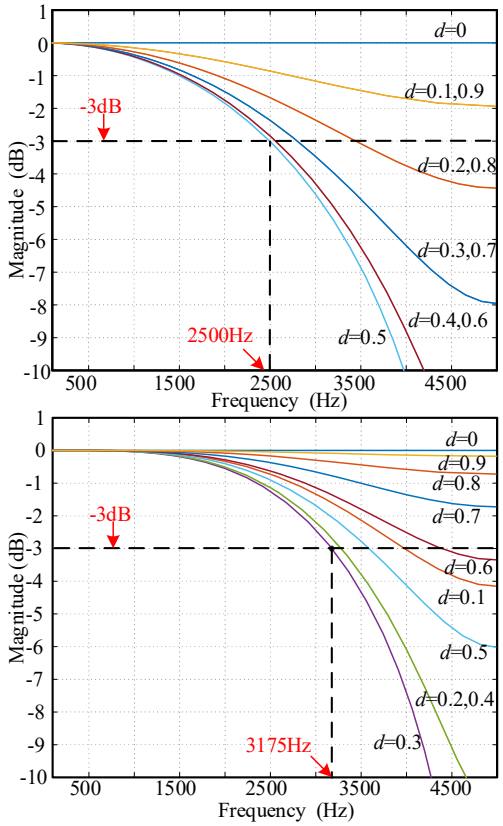

Fig. 4. Amplitude response of first-order and second-order FD filters based on Taylor series expansion

C. *Stability analysis and parameter design of FAMRC*

a) Stability analysis: the steady state error of FAMRC system is obtained from Fig. 3.

$$\begin{aligned} E(z_{\mathrm{m}}) &= \frac{\left(\mathrm{i}_{ref}(z_m) - u_g(z_m)\right)}{1 + \left(G_{rc}(z_m) + 1\right) \cdot G_{\mathrm{op}}(z_m)} \\ &= \left(\mathrm{i}_{ref}(z_m) - u_g(z_m)\right)(1 + G_{pi}(z_m)P(z_m))^{-1} * \\ &\quad \frac{(1 - z_m^{-D} G_d(z_m) Q(z_m))}{(1 - z_m^{-D} G_d(z_m) Q(z_m)(1 - k_r z^m S(z) G_{cl}(z_m)))} \end{aligned} \tag{12}$$

Where, $G_{cl}(z_m) = G_{pi}(z_m)P(z_m) / (1 + G_{pi}(z_m)P(z_m))$, is the closed-loop transfer function of the system before RC is inserted. FAMRC system is stable when the following two conditions are satisfied

(1) the roots of the $1 + G_{pi}(z_m)P(z_m) = 0$ are in the unit circle.

(2) $| z_m^{-D} G_d(z_m) Q(z_m)(1 - k_r z_m^k S(z_m) G_{cl}(z_m)) | < 1$,
$\forall z = e^{j\omega T_m}, 0 < \omega < \pi / T_m$.

It is known that stability condition 1 has nothing to do with FD. For condition 2,

$$\begin{aligned} &| Q(z_m)(1 - k_r z_m^k S(z_m) G_{cl}(z_m)) | < | z_m^{-D} G_d(z_m)^{-1} | \\ &\forall z = e^{j\omega T_m}, 0 < \omega < \pi / T_m \end{aligned} \tag{13}$$

Within the bandwidth of the FD filter, $|z_m^{-D} G_d(z_m)|^{-1} \rightarrow 1$, the stability of the system is independent of the FD filter.

b) Parameter design: the parameters of LCL single-phase grid-connected inverter system are shown in Table1. The sampling factor m is set to 2, Select filter $F_1(z) = F_2(z) = 0.15 z^{-1} + 0.7 + 0.15z$, the cut-off frequency is $2\pi*2460 < 2\pi*2500 = \pi / T_m$.

According to [7] , the parameters of PI controller are designed and calculated. $k_p = 10$, $k_i = 1300$. $G_{cl}(z_m)$ has a amplitude margin of 9.95dB and a phase margin of 154°. $Q(z_m)$ usually selects the low-pass filter with gain less than 1 or constant less than 1 to improve the stability of RC. In this paper, $Q(z_m) = 0.25z_m + 0.5 + 0.25z_m^{-1}$. In order to make $G_{cl}(z_m)$ have faster amplitude attenuation at high frequencies, select the fourth-order Butterworth low-pass filter $S(z_m)$ with cut-off frequency of 1 kHz.The expression of $S(z_m)$ is as follows

$$S(z_m) = \frac{0.04658z_m^4 + 0.1863z_m^3 + 0.2795z_m^2 + 0.1863z_m + 0.04658}{z_m^4 - 0.7812z_m^3 + 0.68z_m^2 - 0.1827z_m + 0.03012} \tag{14}$$

In order to determine the phase lead order k, the Bode diagram of $z_m^k S(z_m)G_{cl}(z_m)$ at 3, 4, 5, 6 is given in Fig.5. It can be seen that when $k = 4$, the phase of $S(z_m)G_{cl}(z_m)$ is close to 0 ° within 1kHz, and the compensation effect is the best.

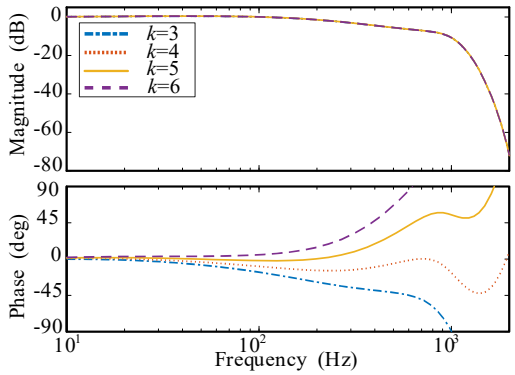

Fig. 5. The amplitude-frequency and phase-frequency characteristics of $S(z_m)G_{cl}(z_m)$ when k takes different values

Finally, select k_r according to condition 2. According to (13)

$$|Q(z_m)(1 - k_r z_m^k S(z_m)G_{cl}(z_m))| < 1, \forall z = e^{j\omega T_m}, 0 < \omega < \pi / T_m \tag{15}$$

Define $H(z_m) = Q(z_m)[1 - k_r z_m^k S(z_m)G_{cl}(z_m)]$, $z_m = e^{j\omega Tm}$. Then when the locus of $H(e^{j\omega Tm})$ is in the unit circle, the system is stable. From Fig.6, when $k_r = 1$, the low frequency region of $H(e^{j\omega Tm})$ is closer to the center of the unit circle.

IV. Simulation Analysis

In order to verify the performance of FAMRC system, the LCL-type single-phase grid-connected inverter model is built in MATLAB/Simulink simulation environment, and the steady-state and dynamic performance are compared with CRC. The reference current is 10A. CRC system, that is, sampling factor $m = 1$, sampling frequency $f_s = 10$kHz, delay beat $N = f_s / f_g$, phase lead order $k = 8$, other parameters remain unchanged.

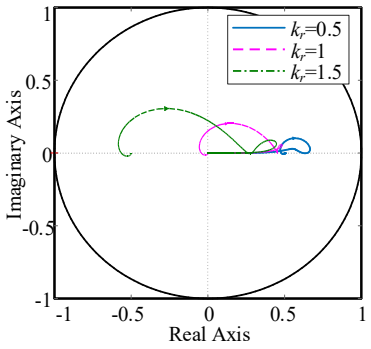

Fig. 6. The trajectory of $H(e^{j\omega Tm})$ when k_r takes different values

A. Steady-state performance

As can be seen from Fig. 7, when $f_g = 50$Hz, $N = T_g / T_s = 200$, $N_m = T_g / T_m = 100$, the output voltage and current waveforms of CRC and FAMRC are almost sinusoidal, the THD of CRC and FAMRC are 0.97% and 1.33% , respectively, both of them can effectively suppress the harmonic in the power grid.

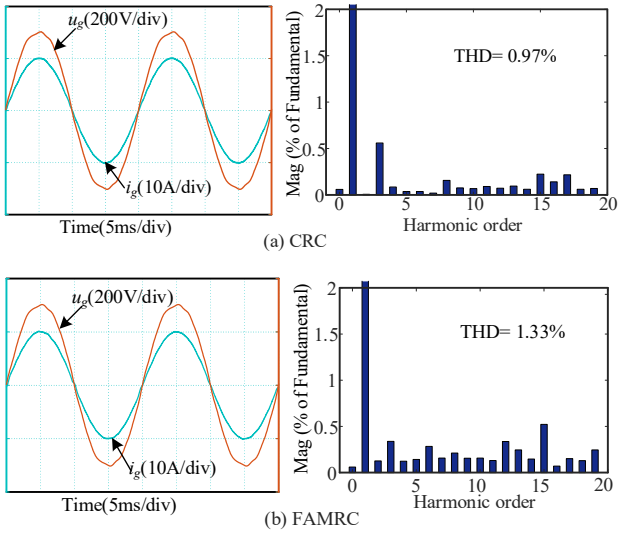

Fig. 7. Voltage and current waveforms and output current spectrum of the two control systems with integer delay ($f_g = 50$Hz)

Fig. 8 and Fig. 9 show that when $f_g = 49.6$Hz, $N = T_g / T_s = 201.6$, $N_m = T_g / T_m = 100.8$; when $f_g = 50.4$Hz, $N = T_g / T_s = 198.4$, $N_m = T_g / T_m = 99.2$, the voltage and current waveform and output current spectrum of CRC and FAMRC control systems under fractional delay are obtained. When $f_g = 49.6$Hz, the THD of CRC and FAMRC are 2.71% and 1.26%, respectively. When $f_g = 50.4$Hz, the THD of CRC and FAMRC are 3.33% and 1.19%, respectively. It can be seen that when fractional delay occurs, the output current waveform of CRC is seriously distorted and the harmonic content is high. The output current waveform of FAMRC is still a smooth sine curve, and the harmonic suppression ability is significantly improved compared with CRC.

Table II shows the THD comparison of the output currents of CRC and FAMRC control systems at different grid frequencies, which can be maintained within 5%. However,

when the grid frequency fluctuates within ±0.4Hz, the THD of CRC is much higher than that of FAMRC, indicating that FAMRC has better frequency adaptability.

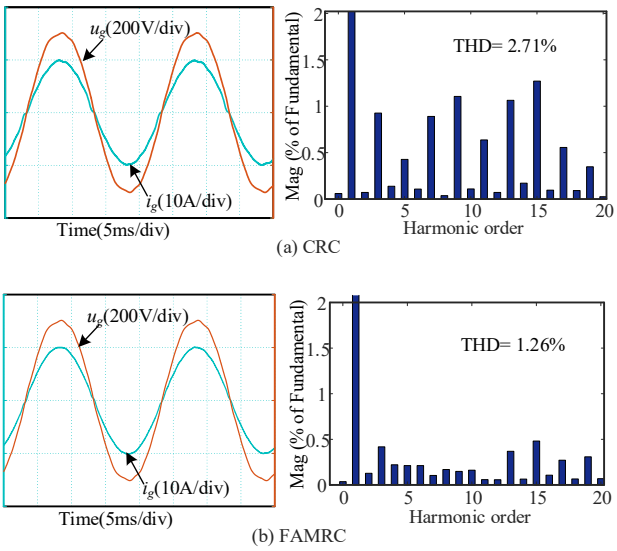

Fig. 8. Voltage and current waveforms and current spectrum analysis of the two control systems at fractional delay (f_g = 49.6Hz)

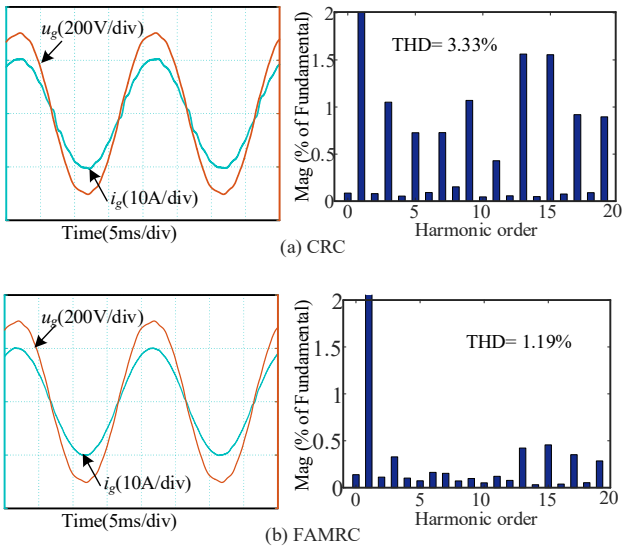

Fig. 9. Voltage and current waveforms and current spectrum analysis of the two control systems at fractional delay (f_g = 50.4Hz)

TABLE II. THD COMPARISON OF OUTPUT CURRENT OF TWO CONTROL SYSTEMS UNDER DIFFERENT GRID FREQUENCIES

Fundamental frequency(Hz)	**THD**		
	CRC	***FAMRC with 2th order proposed FD filter***	***FAMRC with 3th order FIR***
49.6	2.71%	1.26%	1.27%
50	0.97%	1.33%	1.33%
50.4	3.33%	1.19%	1.21%

B. Dynamic Performance

Fig. 10 and Fig. 11 show the dynamic performance of CRC and FAMRC control systems when the grid frequency fluctuates. When f_g = 49.6Hz, the error convergence time of CRC is 0.1s, and the steady-state error of current is 1A; the error convergence time of FAMRC is 0.08s, and the steady-state error is 0.3A. Similarly, when f_g = 50.4 Hz, the error convergence time of CRC is 0.08s, and the steady-state error of current is 1.1A ; the error convergence time of FAMRC is 0.1s, and the steady-state error is 0.3A. It can be seen that when the grid frequency fluctuates, FAMRC and CRC have similar error convergence speed, but can effectively reduce the error.

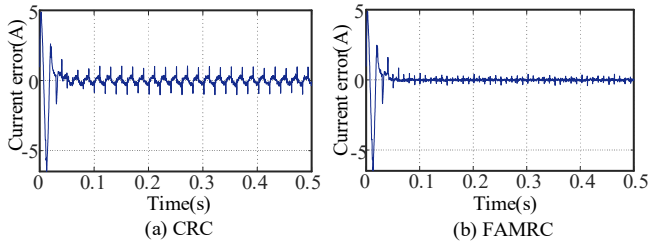

Fig. 10. Current error of two control systems with grid frequency fluctuation (f_g = 49.6Hz)

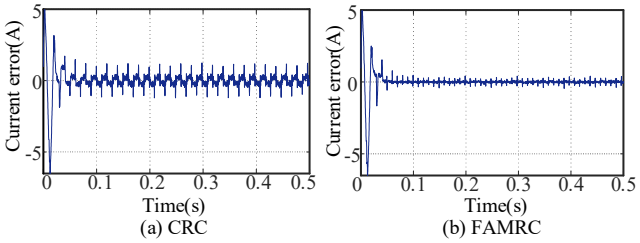

Fig. 11. Current error of two control systems with grid frequency fluctuation (fg = 50.4Hz)

V. CONCLUSION

In order to improve the adaptability of CRC in power grid frequency fluctuation and reduce the computational burden of digital system, a FAMRC strategy is adopted. Through theoretical analysis and simulation, it is verified that FAMRC has similar steady-state and dynamic performance with CRC while reducing digital memory. The Farrow structure FD based on Taylor series expansion can effectively adapt to the change of power grid frequency, ensure higher tracking accuracy and lower THD.

REFERENCES

[1] J. M. Guerrero, F. Blaabjerg, T. Zhelev,K. Hemmes, E. Monmasson, S. Jemei, M. P. Comech, R. Granadino, and J. I. Frau, ``Distributed generation: toward a new energy paradigm," IEEE Industrial Electronics Magazine, vol. 4, no. 1, pp. 52-64, March 2010.

[2] Y. Cai, Y. He, H. Zhou and J. Liu, "Active-Damping Disturbance-Rejection Control Strategy of LCL Grid-Connected Inverter Based on Inverter-Side-Current Feedback," in IEEE Journal of Emerging and Selected Topics in Power Electronics, vol. 9, no. 6, pp. 7183-7198, Dec. 2021.

[3] X. Ding, R. Xue, T. Zheng, F. Kong and Y. Chen, "Robust Delay Compensation Strategy for LCL-Type Grid-Connected Inverter in Weak Grid," in IEEE Access, vol. 10, pp. 67639-67652, 2022.

[4] Q. Zhao and Y. Ye, "A PIMR-type repetitive control for a grid-tied inverter: structure, analysis, and design," in IEEE Transactions on Power Electronics, vol. 33, no. 3, pp. 2730-2739, March 2018.

[5] B. Zhang, K. Zhou and D. Wang, "Multirate repetitive control for PWM DC/AC converters," in IEEE Transactions on Industrial Electronics, vol. 61, no. 6, pp. 2883-2890, June 2014.

[6] B. Han, J. -S. Lai and M. Kim, "Down-Sampled Repetitive Controller for Grid-Connected Ćuk CCM Inverter," in IEEE Journal of Emerging and Selected Topics in Power Electronics, vol. 10, no. 1, pp. 1125-1137, Feb. 2022.

[7] C. Xie, X. Zhao, M. Savaghebi, L. Meng, J. M. Guerrero and J. C. Vasquez, "Multirate fractional-order repetitive control of shunt active power filter suitable for microgrid applications," in IEEE Journal of Emerging and Selected Topics in Power Electronics, vol. 5, no. 2, pp. 809-819, June 2017.

[8] W. Wang, W. Lu, K. Zhou and Q. Fan, "Fractional-order new generation of nk ± m-order harmonic repetitive control for PWM converters," in IEEE Access, vol. 8, pp. 180706-180721, 2020.

[9] Q. Zhao, H. Zhang, Y. Gao, S. Chen and Y. Wang, "Novel Fractional-Order Repetitive Controller Based on Thiran IIR Filter for Grid-Connected Inverters," in IEEE Access, vol. 10, pp. 82015-82024, 2022.

[10] M. Jamil, A. Waris, S. O. Gilani, B. A. Khawaja, M. N. Khan and A. Raza, "Design of robust higher-order repetitive controller using phase lead compensator," in IEEE Access, vol. 8, pp. 30603-30614, 2020.

[11] G. Escobar, P. Mattavelli, M. Hernandez-Gomez and P. R. Martinez-Rodriguez, "Filters with linear-phase properties for repetitive feedback," in IEEE Transactions on Industrial Electronics, vol. 61, no. 1, pp. 405-413, Jan. 2014.

[12] W. Liao, Y. Sun, Q. Zhao and S. Chen, "Double-fractional OPIMR controller for a single-phase grid-tied inverter," 2021 IEEE 10th Data Driven Control and Learning Systems Conference (DDCLS), 2021, pp. 871-876.

[13] C. Zeng, S. Li, H. Wang and H. Miao, "A fractional phase compensation scheme of PRMRC for LCL inverter connected to weak grid," in IEEE Access, vol. 9, pp. 167027-167038, 2021.

[14] T. Moller, R. Machiraju, K. Mueller and R. Yagel, "Evaluation and design of filters using a Taylor series expansion," in IEEE Transactions on Visualization and Computer Graphics, vol. 3, no. 2, pp. 184-199, April-June 1997.

[15] C. W. Farrow, "A continuously variable digital delay element," in IEEE International Symposium on Circuits and Systems, 1988, pp. 2641-2645 vol.3.

[16] R. Nazir, A. Wood, H. Laird and N. Watson, "An adaptive repetitive controller for three-phase PWM regenerative rectifiers," International Conference on Renewable Energy Research and Applications (ICRERA), 2015, pp. 1126-1131.

[17] V. Valimaki, "A new filter implementation strategy for Lagrange interpolation," in International Symposium on Circuits and Systems, 1995, pp. 361-364 vol.1.

First Author Kaiyue Liu	**Position:** Ms.
	Research Field: Inverter control and repetitive control theory
	Homepage URL:
Second Author Qiangsong Zhao	**Position:** Assoc. Prof
	Research Field: Inverter control method, repetitive control
	Homepage URL:
Third Author Gong Zhang	**Position:** Mr.
	Research Field: Inverter control and repetitive control theory
	Homepage URL:
Fourth Author Bin Wang	**Position:** Mr.
	Research Field: Repetitive control theory and active damping control strategy
	Homepage URL: